

## Temperature dependence of microwave characteristics of $n^{++}np^{++}$ Si IMPATT diode at X band

Pankaj De

Department of Physics, Gobardanga Hindu College, West Bengal State University, India

---

**Abstract:** The dependence of both microwave negative resistance ( $R$ ) and its positive series resistance ( $R_s$ ) on the rise of diode junction temperature in the range of  $100^\circ\text{C}$  to  $220^\circ\text{C}$  of HP  $n^{++}np^{++}$  Si IMPATT [1] diode with flat doping density ( $7 \times 10^{21} \text{ m}^{-3}$ ) at X band (8-12) GHz have been simulated. The studies followed by Gummel-Blue Technique [2] show that for a constant experimental bias current of 25 mA [1], for which the space charge effect is not prominent, the value of negative conductance and negative resistance degrade taking into account the changes in the ionization rates and drift velocities due to rise of temperature. As a result, it is observed that the series resistance increases with the increase of temperature.

**Keywords:** Negative microwave resistance, IMPATT diode, Series Resistance, X Band

---

### I. Introduction

The rise of p-n junction temperature and its burning problem are crucial in IMPATT (IMPact ionization Avalanche Transit Time) mode operation. The input power of the diode is partly used for conversion into microwave energy and partly for heating the diode. It is known that the positive series resistance contributes major role for the Joule heat dissipation and degrades overall microwave performance of avalanche transit time diode. As junction temperature increases, the reverse saturation current rises exponentially and leads to thermal runaway. Also, the complete removal of the junction heat is difficult using available good heat sink. Therefore, microwave and mm wave power devices generally operate at temperatures above the ambient. The increased reverse saturation current produces a faster build up of the avalanche current and degrades the negative resistance of the device.

Intrinsic IMPATT operation depends directly on the temperature and the work of Dalle et al [3] clearly indicates the decrease of RF power with the increase of temperature. The power loss due to unswept epitaxy can be reduced in punched through structures. Both the electron and hole transport parameters are decreasing functions of temperature [4]. According to Ray et al [5] depletion layer width, ionization rate and saturation drift velocity are sensitive to the junction temperature. Even in pulse mode the junction temperature and these three parameters vary during the pulse width, resulting in large signal impedance variation within the pulse. This time varying device impedance causes frequency chirp in pulsed impatt oscillators [5].

The value of  $R_s$  basically depends on the width of the undepleted region, which is very difficult to measure under oscillating condition, because the electric field distribution is a function of time, temperature, current density, doping etc. Its direct measurement by a network analyzer is also difficult due to circuit modeling difficulties [6]. The optimum transfer of the emitted RF power to the load circuit depends on the total loss resistance  $R_s$ , which also strongly depends on the choice of both the dc bias current density and the diode area.

The positive series resistance has to be kept to the minimum value to obtain oscillating power from the device. In 1983, Adlerstein et al [7] proposed a technique of measuring  $R_s$  from the threshold current and threshold frequency for double drift region GaAs material considering equal ionization rates and drift velocities of the charge carriers. In 1993, Mitra et al [1] calculated  $R_s$  for Si IMPATT diode by a choice of multiplier to the unequal ionization rates of electrons and holes, where field dependence of the drift velocities and temperature dependence of ionization rates have been neglected.

The author [8-11] simulated the values of  $R_s$  for Si  $n^{++}np^{++}$  HP X band IMPATT diode at  $100^\circ\text{C}$  following generalized AC analysis of Gummel and Blue [2], where temperature variation has been neglected. But in the present analysis the author has been able to study the change in the value of  $R_s$  with temperature in the realistic range of  $100$ - $220^\circ\text{C}$  considering the change in ionization rates and drift velocities [12-13], experimental threshold current density, peak operating frequency at X band and high multiplication factor ( $10^6$ ) [14-15] for electron and hole which corresponds to very low reverse saturation current.

### II. Numerical Approach

#### a. Ionization parameters

It is found that impact ionization is suppressed by increasing temperature because of the increase in phonon scattering [16-17]. The impact ionization process depends on temperature, largely via scattering from

optical phonons. This phenomenon is conventionally described in terms of coefficients  $\alpha$  and  $\beta$  for electrons and holes respectively, which are the reciprocal of the mean distance between successive ionization events. The temperature dependence of  $\alpha$  reduces with increasing field, essentially because carriers scatter less often during corresponding shorter ionization path lengths. At a given electric field, the ionization rate decreases with increasing temperature [18]. W. N Grant reported [12] field dependence of ionization rates of electrons and holes at 22°C in Si by an exponential form given by

$$\alpha_{n,p}(x) = A_{n,p} \exp\left[-\frac{B'_{n,p}}{E(x)}\right]$$

It was also observed that the changes in  $\alpha_n$  and  $\alpha_p$  with temperature [13] could be incorporated by using temperature dependent values of  $B'_n$  and  $B'_p$ . Where temperature coefficient of  $B'_n$  and  $B'_p$  are given by

$$\frac{\partial(B'_n)}{\partial T_j} = 1.3 \times 10^5 \text{ Vm}^{-1} \text{ C}^{-1}$$

$$\frac{\partial(B'_p)}{\partial T_j} = 1.1 \times 10^5 \text{ Vm}^{-1} \text{ C}^{-1}$$

Thus in the field range of  $(2.4 \text{ to } 5.3) \times 10^7 \text{ V m}^{-1}$ , the values of  $\alpha_n$  and  $\alpha_p$  are calculated at different temperatures using the following expressions,

$$\alpha_n(E, T_j) = 6.2 \times 10^7 [\exp\{-(1.08 \times 10^8 + 1.3 \times 10^5 (T_j - 22)) / E\}]$$

$$\alpha_p(E, T_j) = 2.0 \times 10^8 [\exp\{-(1.97 \times 10^8 + 1.1 \times 10^5 (T_j - 22)) / E\}]$$

For field range between  $(5.3 \text{ to } 7.7) \times 10^7 \text{ V m}^{-1}$  the ionization rates are given by

$$\alpha_n(E, T_j) = 5.0 \times 10^7 \exp[-(9.9 \times 10^7 + 1.3 \times 10^5 (T_j - 22)) / E]$$

$$\alpha_p(E, T_j) = 5.6 \times 10^7 \exp[-(1.32 \times 10^8 + 1.1 \times 10^5 (T_j - 22)) / E]$$

Where  $T_j$  is the junction temperature expressed in degree centigrade.

### b. AC analysis

The static properties of the diode have been obtained following the method of Datta et al [18]. With the static parameters as input, the spatial variation of diode negative resistivity (R) and the reactivity (X) in the depletion layer have been obtained solving the following device equations [2], [10], [14], [19] and [20]

$$\frac{\partial^2 R}{\partial x^2} + \{\alpha_n(x) - \alpha_p(x)\} \frac{\partial R}{\partial x} - 2\bar{r} \frac{\omega}{\bar{v}} \frac{\partial X}{\partial x} + \left\{ \frac{\omega^2}{\bar{v}^2} - H(x) \right\} R - 2\bar{\alpha}(x) \frac{\omega}{\bar{v}} R - \frac{2\bar{\alpha}(x)}{\bar{v}\epsilon} = 0$$

And

$$\frac{\partial^2 X}{\partial x^2} + \{\alpha_n(x) - \alpha_p(x)\} \frac{\partial X}{\partial x} + 2\bar{r} \frac{\omega}{\bar{v}} \frac{\partial R}{\partial x} + \left\{ \frac{\omega^2}{\bar{v}^2} - H(x) \right\} X + 2\bar{\alpha}(x) \frac{\omega}{\bar{v}} R + \frac{\omega}{\bar{v}^2 \epsilon} = 0$$

Replacing the diode impedance  $R+jX$  by  $Z$ , the total integrated negative resistivity ( $Z_R$ ) and reactivity ( $Z_X$ ) of the diode at the operating frequency ( $f$  where  $\omega=2\pi f$ ) and temperature can be determined from the numerical integration of the resistivity and reactivity profiles over the depletion layer as follow-

Where  $W$  is the depletion layer width of the  $n^{++}np^{++}$  structure.

Hence, the diode total negative conductance ( $G_D$ ) and susceptance ( $B_D$ ) are obtained as follow-

$$Z_R(\omega, T) = \int_0^W R \cdot dx$$

$$Z_X(\omega, T) = \int_0^W X \cdot dx$$

$$G_D(\omega, T) = -\frac{Z_R}{(Z_R)^2 + (Z_X)^2}$$

$$B_D(\omega, T) = \frac{Z_X}{(Z_R)^2 + (Z_X)^2}$$

Where,  $G_D$  and  $B_D$  are functions of RF voltage ( $V_{RF}$ ) and frequency such that the steady state condition for oscillation is given by [2], [7], and [10],

$$g_L(\omega, T) = -G_D(\omega, T) - \{B_D(\omega, T)\}^2 R_s(\omega, T)$$

Under the dynamic condition  $V_{RF}$  is small and  $R_s$  can be calculated by considering the value of load conductance ( $g_L$ ), which is nearly equal to the diode conductance ( $G_D$ ) at resonance.

### III. Results and discussion

#### a. Static properties

The electric field profiles at breakdown of the  $n^{++}np^{++}$  single drift region (SDR) Si diode at different operating temperatures have shown in Fig.1. It shows that the maximum electric field at the junction and the punch through condition increases with the rise of temperature. As a result, the avalanche region and the effective width of the diode increase with temperature. At 100°C the diode is just punch through, which is the required field profile for optimum performance [10]. The linear rise of the electric field in the depletion zone indicates that the diode is free from severe space charge effect at experimental bias current of 25 mA. The field value in the depletion layer increases as the ionization rate decreases with the rise of temperature. The avalanche region, drift region and the total dc breakdown voltage  $V_A$ ,  $V_D$  and  $V_B$  respectively increase with temperature. But the dc to microwave conversion efficiency ( $\eta$ ) estimated from the Scharfetter-Gummel formula [21] indicates a minor change with temperature.

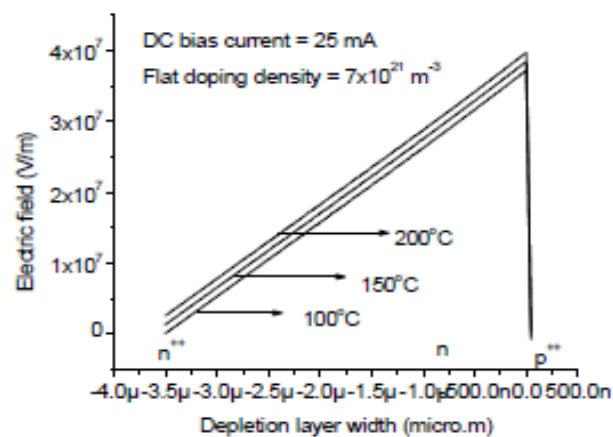


**Fig. 1.** Electric field distribution in the depletion layer of X band Si  $n^{++}np^{++}$  IMPATT diode at different operating temperatures under same bias current (25 mA)

The normalized current density difference of hole and electron ( $J_p - J_n$ )/ $J_{dc}$  i.e. the  $P(x)$  profile, shown in Fig. 2, indicates the position of the avalanche center in the depletion zone, where  $J_p = J_n$ , i.e.  $P(x) = 0$ ; and also the width of the avalanche and drift zone. From the studies of the  $P(x)$  profiles (not shown in Fig.2), it is observed that the avalanche region width increases negligibly with temperature, but the increasing electric field in the avalanche zone (as shown in Fig. 1) increases the value of  $V_A$  and  $V_D$  with temperature. The dc power input ( $P_{dc}$ ) and the expected ac output power ( $P_{ac}$ ) have been calculated from the Sharfetter-Gummel formula [21] and are given in Table 1. It is found that the experimentally observed ac power as obtained by Mitra et al [1], is of the order of 100 mW, which is nearly one sixth of the present theoretical result. The present dc analysis suggests an increase in  $P_{dc}$  with the rise of temperature, which is also a usual expectation.

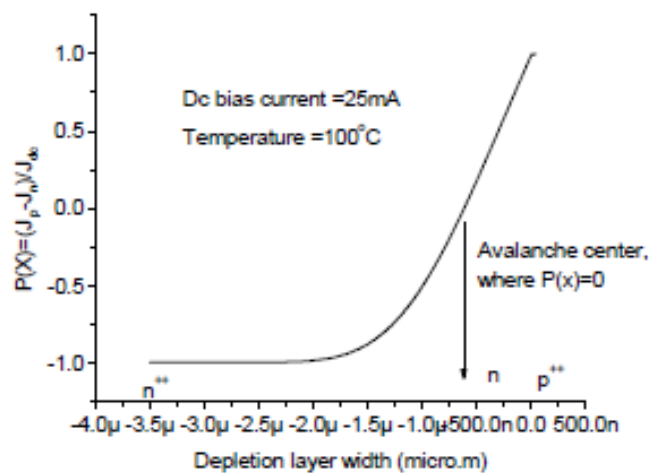


**Fig.2.** Normalized current density difference i.e.  $(J_p - J_n) / J_{dc}$  or  $P(x)$  profile in the depletion region of X band Si  $n^{++}np^{++}$  IMPATT diode.

**Table 1:** The dc properties of  $n^{++}np^{++}$  Si X band IMPATT diode at bias current 25 mA with diode cross sectional area  $7.25 \times 10^{-9} \text{ m}^2$  and at different temperatures.

Temperature (°C)	$V_A$ (V)	$V_D$ (V)	$V_B$ (V)	$\eta$ %	Input dc power (Watt)	Output ac power (Watt)
100	47.2	65.5	113	18.5	2.825	0.522
110	47.3	66.3	114	18.6	2.850	0.530
120	48.1	67.1	115	18.5	2.875	0.531
130	49.0	68.0	117	18.5	2.925	0.548
140	49.2	69.0	118	18.6	2.950	0.558
150	49.9	69.9	120	18.6	3.000	0.570
170	50.5	71.7	122	18.7	3.050	0.570
180	51.9	72.5	124	18.7	3.100	0.579
190	51.9	73.4	125	18.7	3.125	0.581
200	53.1	74.3	127	18.6	3.175	0.590
210	53.7	75.1	129	18.6	3.225	0.599
220	54.3	76.1	130	18.6	3.250	0.604

**b. Dynamic properties**

The negative resistivity profiles in the active region of the diode under the same operating bias current (25 mA) and frequency (10 GHz), but at different temperatures have been plotted in Fig. 3. The spatial distribution of the negative resistivity in the depletion layer gives a clear insight regarding the microwave power generation in the avalanche and drift region which is the significant characteristics of the AC analysis of Gummel and Blue [2]. The profiles indicate that the drift region contribute maximum negative resistance compared to its avalanche zone. The diode yields maximum negative resistance at 100°C and the same decreases with the rise of temperature. It is also observed from Fig. 3 that the substrate-epitaxy ( $nn^{++}$ ) interface region contributes lowest value of negative resistance (R). As the temperature increases from 100°C to 200°C, the value of negative resistance decreases from  $-11.65\Omega$  to  $-8.25\Omega$ , as given in Table 2.

**Table 2:** The small signal properties of  $n^{++}np^{++}$  Si X band IMPATT diode at bias current 25 mA and operating frequency 10 GHz, but at different temperatures.

Temperature (°C)	(-G) $10^4$ mho.m <sup>-2</sup>	B $10^5$ mho.m <sup>-2</sup>	(-R) Ohm	$R_s$ ohm	$g_L$ $10^4$ mho.m <sup>-2</sup>
100	37.55	18.28	11.65	1.25	34.5
110	33.74	19.46	9.34	1.30	30.15
120	32.18	19.49	8.90	1.37	28.4
130	31.15	19.46	8.67	1.41	27.28
140	30.73	19.41	8.59	1.47	26.71
150	30.37	19.34	8.56	1.53	26.20
170	29.62	19.2	8.44	1.68	25.10

180	29.09	19.17	8.35	1.79	24.3
190	28.77	19.12	8.31	1.87	23.80
200	28.56	19.08	8.29	1.95	23.40
210	28.20	19.02	8.23	2.13	22.60
220	28.14	18.98	8.25	2.23	22.30

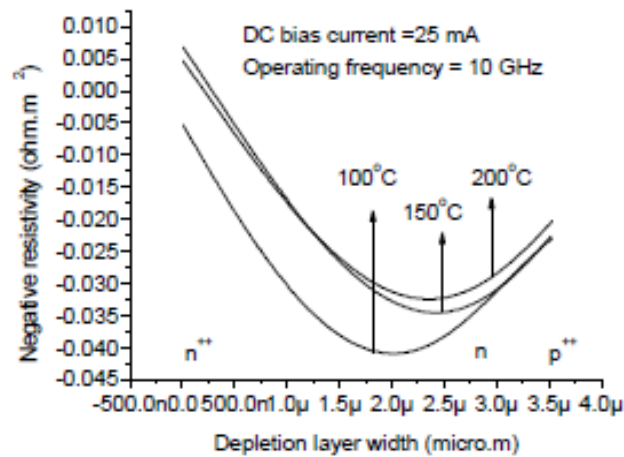


**Fig. 3.** Negative resistivity profiles in the depletion layer of X band  $n^{++}np^{++}$  Si IMPATT diode at different temperatures.

The frequency dependence of negative conductance (G) and positive susceptance (B) at a constant bias current of 25 mA but at different temperatures had shown in Fig. 4. It shows that the maximum (center) negative conductance and the corresponding center frequency ( $f_c$ ) decrease with the increase of temperature as expected, which is defined as the frequency chirp [22] in avalanche transit time devices. The decrease of center frequency is due to the widening of the effective depletion width as a result of increasing temperature. The Fig. 4 also suggests that the present SDR diode with active layer doping  $7 \times 10^{21}/m^3$ , operating at 25 mA dc bias current and ambient temperature  $100^\circ C$  operate exactly at X band, with center frequency at 11 GHz. The present decrease in the center frequency due to rise of temperature is in contrary with the published data [10], where the higher field value in the  $nm^{++}$  (substrate-epitaxy) interface indicating higher punched through and lower field value at the  $p^{++}n$  junction due to lower active zone doping result upward shift in the center frequency. The decrease of negative conductance with temperature has been plotted in Fig. 5. The rate of decrease is more in the range  $100^\circ C$  to  $130^\circ C$ .

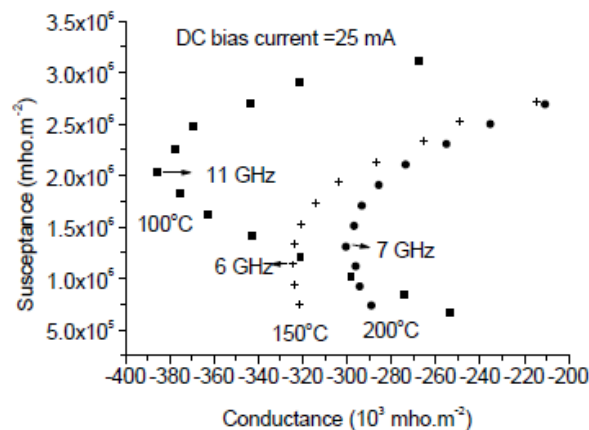


**Fig.4.** Admittance (Conductance-Susceptance) characteristics at different operating temperatures of X band Si  $n^{++}np^{++}$  IMPATT diode.

The diode yields higher negative resistance (8-10  $\Omega$ ) compared to the series resistance (1.22-2.1  $\Omega$ ), which is the required condition for sustained oscillation. Fig. 6, indicates an approximate linear rise of  $R_s$  with device temperature within the realistic limit of 2  $\Omega$  for X band IMPATT diode [1].

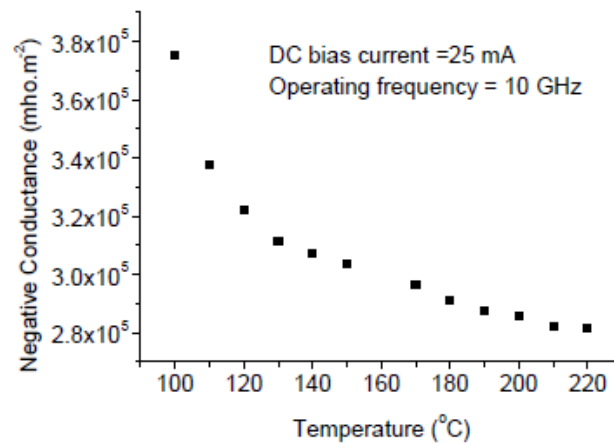


Fig.5. Temperature variation of negative conductance of X band Si  $n^{++}np^{++}$  IMPATT diode.

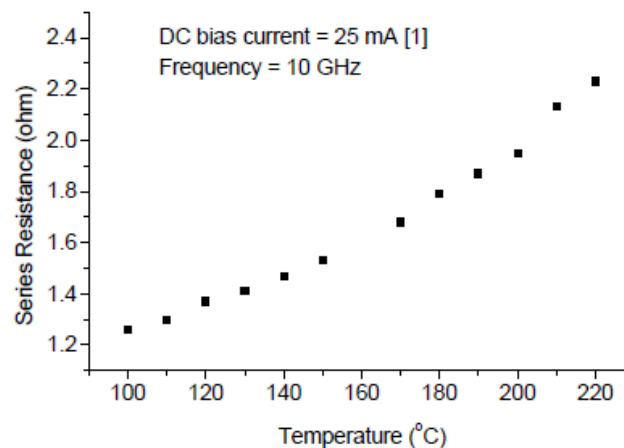


Fig. 6. Temperature-Series Resistance profile of X band Si  $n^{++}np^{++}$  IMPATT diode

#### IV. Conclusions

The present studies indicate an overall degradation in the microwave properties of negative resistance and negative conductance of IMPATT diode in the X band due to rise in the operating temperature at a constant bias current and under slight punched through. As a result, the positive series resistance increases with the increase of temperature that may cause an increase in the Joule heat dissipation at higher operating bias current (>25 mA) leading to thermal instability and burnout of the diode. The study also coincides with the earlier results regarding the decrease of operating frequency with the rise of temperature leading to frequency chirp.

#### Acknowledgement

The author acknowledges University Grants Commission, India, for approval of Minor Research Project.

#### References

- [1]. M.Mitra, M. Das, S. Kar, and S. K. Roy, A study of the electrical series resistance of Silicon IMPATT diodes, IEEE Trans Electron Devices, 40, 1993, 1890-1893.
- [2]. H. K. Gummel, and J. L. Blue, A small signal theory of avalanche noise in IMPATT diodes, IEEE Trans. Electron Devices, 14, 1967, 569-580.
- [3]. C. Dalle, P. A. Rolland, and G. Lleti, Flat doping profile double drift silicon IMPATT for reliable CW high power, high efficiency generation in the 94 GHz window, IEEE Trans. Electron Devices, 37, 1990, 227-236.

- [4]. C. Jacoboni, C. Canali, G. Ottaviani, and A. A. Quaranta, A review of some charge transport properties of Si, *Solid State Electron*,20, 1977, 77-82.
- [5]. U. C. Ray and A. K. Gupta, Intrapulse frequency variation in a W band pulsed IMPATT diode, *Microwave Journal*, 1994, 238-244.
- [6]. U. C. Roy, and A. K. Gupta, Measurement of electrical series resistance of W band Si IMPATT diode, *Proc. of the second Asia-Pacific Microwave Conf, Beijing People's Republic of China*, 1998.
- [7]. M. G. Adlerstein, L. H. Holway, and S. L. G. Chu, Measurement of series resistance in IMPATT diodes, *IEEE Trans. Electron Devices*, 30, 1983, 179-182.
- [8]. P. De, Computer simulation of series resistance of an SDR silicon IMPATT diode in the X band, *Int J. Electron*,81, 1996, 545-550.
- [9]. P. De, Effect of current density on the series resistance of SDR ( $n^{++}np^{++}$ ) Silicon IMPATT diode in the X band, *Phys. Stat. Sol(a)*,168, 1998, 549-555.
- [10]. P. De, and P. K. Chakraborty, 2004 Effect of punch through on the microwave series resistance of  $n^{++}np^{++}$  Si IMPATT diodes around the X band, *Semicond. Sci. Technol*, 19 2004, 859-863.
- [11]. P. De, Effect of charge bump on the series resistance and microwave properties of Si  $n^{++}np^{++}$  IMPATT diode at X band, *Indian J Pure & Appl. Phys*, 43, 2005, 794-798.
- [12]. W. N. Grant, Electron and hole ionization rates in epitaxial Silicon, *Solid State Electron*,16, 1973, 1189-1203.
- [13]. C. Canali, G. Ottaviani, and A. A. Quaranta, Drift velocity of electrons and holes and associated anisotropic effects in Silicon, *J. Phys. Chem. Solids*, 32, 1971, 1707-1711.
- [14]. N. Majumder and S. K. Roy, Saturation current induced effects on the microwave and millimeter wave performance of GaAs double drift region IMPATTs, *Int. J. Electron*,71 1991, 227-237.
- [15]. P. De, Optically induced series resistance and microwave properties of  $n^{++}np^{++}$  X band Si IMPATT diode, *Journal of Electronics and Communication Engineering (IOSR-JECE)*, 4, 2014, 46-49.
- [16]. C. Groves, R. Ghin, J. P. R. David and G. J. Rees, Temperature dependence of impact ionization in GaAs, *IEEE Trans. Electron Devices*, 50, 2003, 2027-2031.
- [17]. W. P. Neo and H. Wang, Temperature dependence of the electron impact ionization in InGaP-GaAs-InGaP DHBTs, *IEEE Trans. Electron Devices*,51, 2004, 304-310.
- [18]. S. M. Sze, *Physics of Semiconductor Devices*, 2<sup>nd</sup> edn. (New Delhi: Wiley Eastern) 1991, p. 49.
- [19]. D. N. Datta, S. P. Pati, J. P. Banerjee, B. B. Pal, and S. K. Roy, Computer analysis of DC field and current density profiles of DAR IMPATT diodes, *IEEE Trans. Electron Devices*,29, 1982, 1813-1816.
- [20]. J. P. Banerjee, and S. K. Roy, Design and optimization of the doping profile of double drift low-high-low indium phosphide diodes, *Semicond Sci. Technol*, 6, 1991, 663-669.
- [21]. D. L. Scharfetter, and H. K. Gummel, Large signal analysis of a Si Read Diode oscillator, *IEEE Trans. Electron Devices*, 16, 1969, 64-77.
- [22]. S. K. Roy, *Wiley Encyclopedia of Electrical and Electronics Engineering*, John Wiley & Sons, Inc., 22, 1999, 421-442.